MODIFIED PASCHEN'S LAW FOR MICROSCALE AND NANOSCALE GAPS

Allen L. Garner
BioElectrics and ElectroPhysics Laboratory
School of Nuclear Engineering
School of Electrical and Computer Engineering
Department of Agricultural and Biological Engineering
Purdue University

algarner@purdue.edu

Acknowledgment of Funding Support

- Nuclear Regulatory Commission Nuclear Education Program Faculty Development Grant Program at Purdue University
- Office of Naval Research (Grant No. N00014-17-1-2702).
- Air Force Office of Scientific Research (FA9550-18-1-0218).
- Air Force Office of Scientific Research (FA9550-19-1-0101).
- Directed Energy Professional Society Graduate Scholarship
- Purdue Research Foundation Graduate Fellowship
- Purdue Doctoral Fellowship
- Purdue Summer University Fellowship

Thank you to the students Who Have Worked on This project

- Amanda Loveless (Post-doc, Purdue): Theoretical Development
- Russell Brayfield (PhD, AFRL): Experimental Analysis
- Andrew Fairbanks (Grad Student, NE): Experimental Analysis
- Adam Darr (Grad Student, NE): Quantum breakdown; Space charge theory with collisions; thermionic emission; crossed-field theory.
- Harsha (Grad Student, NE): Variational calculus for space charge limited emission theory
- Sarah Lang (Grad Student, NE): Liquid Emission modeling
- Shengjie Gao (Grad Student, IOE): Imaging of surfaces.
- Sam Dynako (Undergrad, ECE): Error Propagation of theory; Space charge theory with collisions
- Caleb Darr (Undergrad, NE): Experimental Analysis; Theory of Thermionic emission.
- Catherine Darr (Undergrad, AAE): Experimental Breakdown
- Jacqueline Malayter (Undergrad, ECE): Work function modeling for rough surfaces.
- Lorin Breen (Undergrad, NE): Modeling non-uniform microscale gas breakdown.
- Weihang Li (Undergrad, AAE): Experimental Analysis

Motivation

Induce breakdown

- Combustion[1]
- Electric micropropulsion[2]
- Medicine[3]

Prevent breakdown

- For electric pulse applications[4]
- High power microwaves
- Microelectromechanical systems (MEMS) are used in biotechnology, medicine, and communications[5]
- Nanoelectromechanical systems (NEMS) are being studied for sensing and scanning[6]

Plasma Ball:

http://www.real-world-physics-problems.com/plasma-ball.html

Argon Plasma:

https://ysjournal.com/article/rspg-exploration-of-plasma-physics/

[1] Y. Ju and W. Sun, Prog. Energy and Comb. Sci. **48**, 21-83 (2015).
[2] W. P. Wright and P. Ferrer, Prog. Aero. Sci. **74**, 48–61 (2015).
[3] M. Martinez-Sanchez and J. E. Pollard, J. Propul. Power **14**, 688–699 (1998).
[4] A. L. Garner, A. Caiafa, Y. Jiang, S. Klopman, C. Morton, A. S. Torres, A. M. Loveless, and V. B. Neculaes, PLoS ONE, 12(7), e0181214 (2017).
[5] R. Bogue, Sens. Rev. **27**, 7–13 (2007).
[6] H. Craighead, Science **290**, 1532–1535 (2000).

PURDUE UNIVERSITY | School of Nuclear Engineering

Plasma Formation Mechanisms

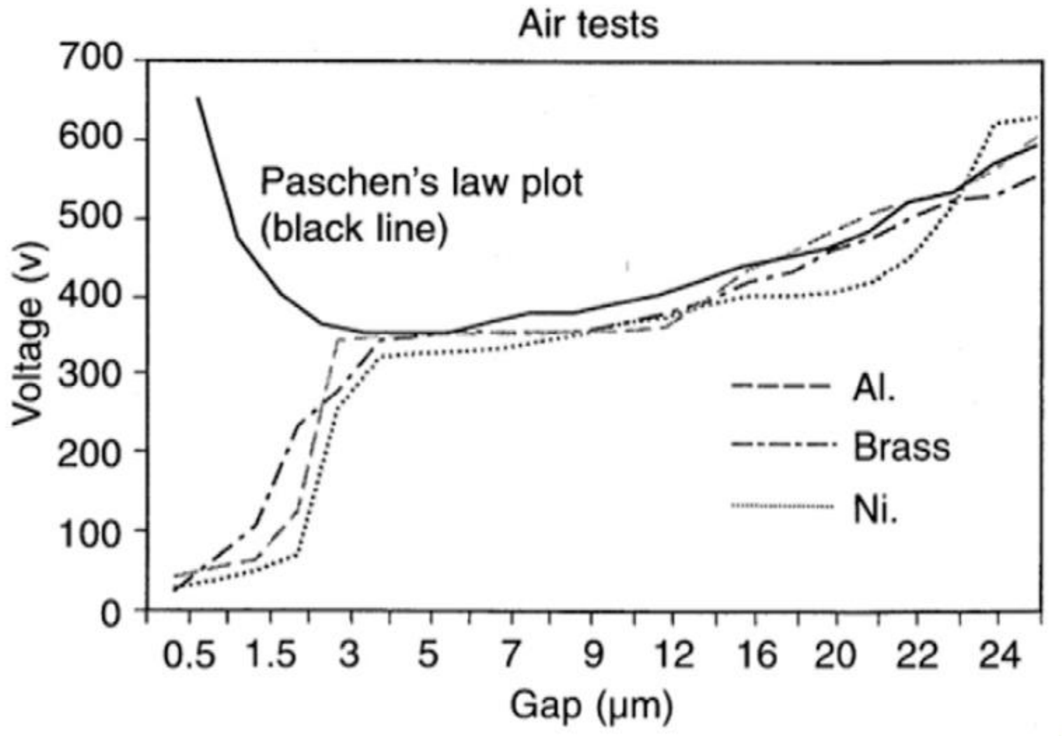

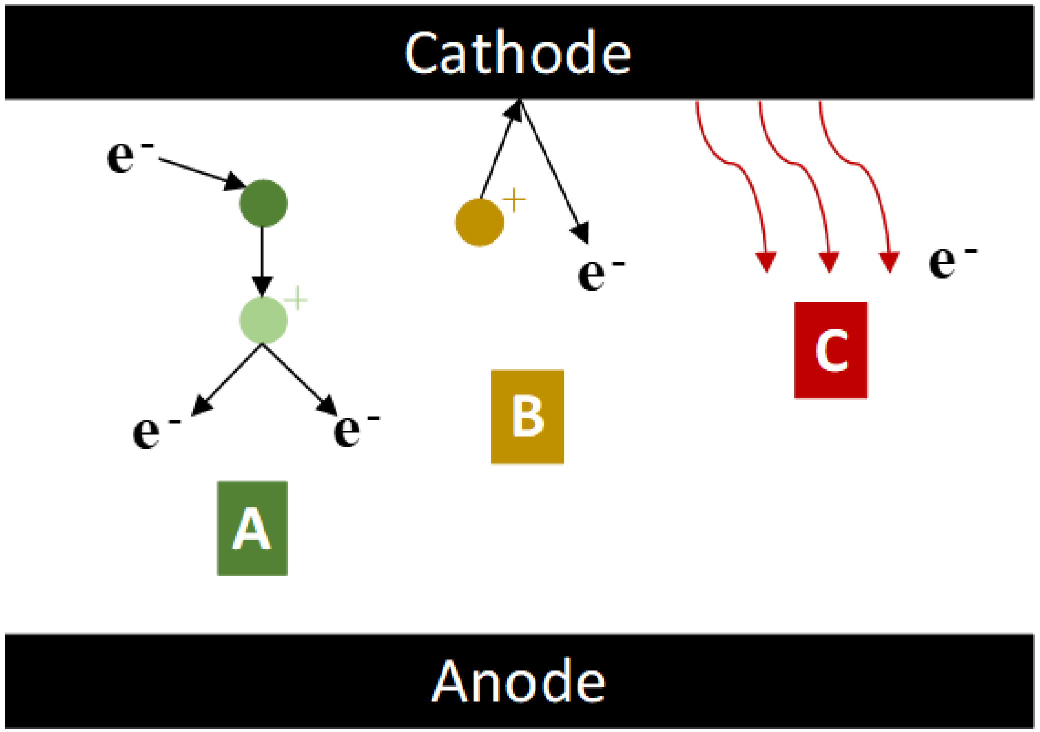

D. B. Go and A. Venkattraman, J. Phys. D **47**, 503001 (2014).
W. S. Boyle and P. Kisliuk, Phys. Rev. **97**, 255-259 (1955).

A: Impact ionization & collisional process – Townsend Avalanche. B: Ion-induced secondary emission; C: Thermo-field emission.

A. L. Garner, A. M. Loveless, J. N. Dahal, and A. Venkattraman, IEEE Trans. Plasma Sci. **48**, 808-824 (2020).

PURDUE UNIVERSITY | School of Nuclear Engineering

Microscale Gas Breakdown

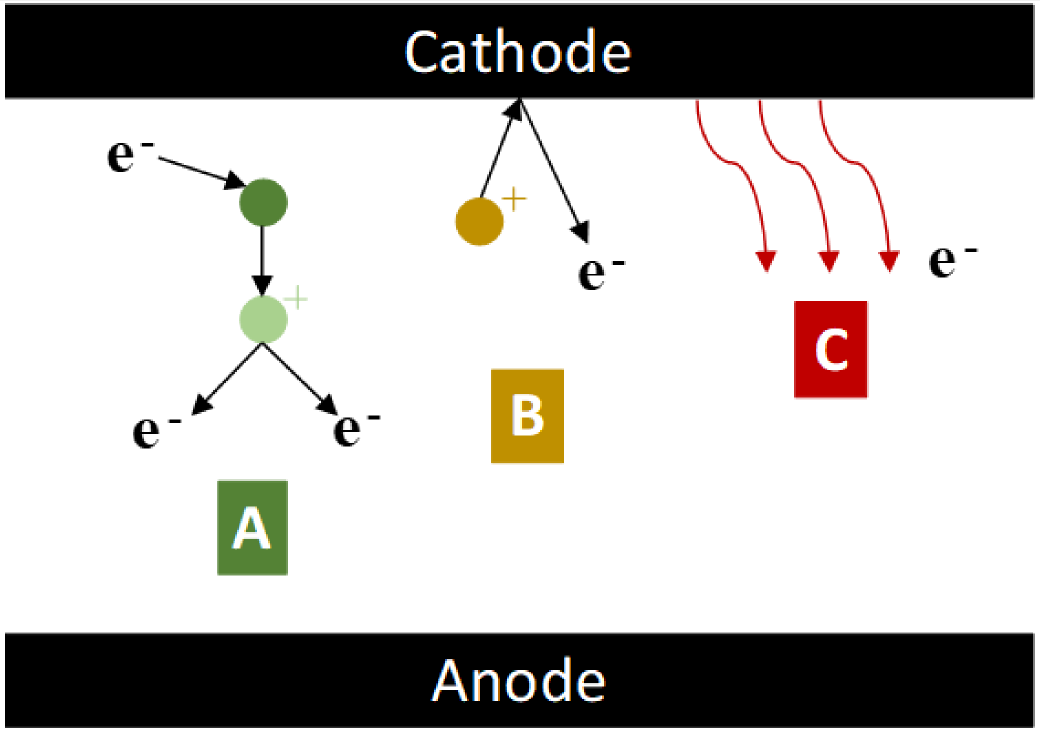

A: Impact ionization & collisional process – Townsend Avalanche. B: Ion-induced secondary emission; C: Field emission.

Modify Townsend avalanche criterion to include ion enhancement from positive space charge due to field emission

$$(\gamma_{SE} + \gamma')[\exp(\alpha d) - 1] = 1$$

This positive space charge will also increase the electric field by an amount $E^+ \ll E$

$$j'_{FN} = C_{FN}(E + E^+)^2 \exp[-D_{FN}/(E + E^+)]$$

Couple with Poisson's equation

$$\frac{dE}{dx} = \frac{\rho}{\varepsilon_0}$$

where ρ is the charge density and ε_0 is the permittivity of free space. At breakdown:

$$F_{br} = \frac{2E^2 v_d \varepsilon_0}{D_{FN} d j_{FN}} \frac{\{1 - \gamma_{SE}[\exp(\alpha d) - 1]\}}{[\exp(\alpha d) - 1]} = \frac{\exp(x_0)\,(1 + 2\bar{E} x_0)}{x_0}$$

$$x_0 = \frac{-1 + \sqrt{1 + 8\bar{E}}}{4\bar{E}} \approx 1$$

A. L. Garner, A. M. Loveless, J. N. Dahal, and A. Venkattraman, IEEE Trans. Plasma Sci. **48**, 808-824 (2020).

Nondimensionalization FOR THE GENERAL CASE

Dimensionless Variables

$$\bar{E} = EE_*^{-1}, \quad \bar{\tau} = T\tau_*^{-1}, \quad \bar{p} = pp_*^{-1}, \quad \bar{d} = dL^{-1},$$
$$\bar{j}_{FN} = j_{FN} j_0^{-1}, \quad \bar{\alpha} = \alpha L, \quad \bar{\phi} = \phi\phi_*^{-1}$$

Scaling Terms

$$p_* = E_* B_p^{-1}, \quad L = p_*^{-1} A_p^{-1}, \quad j_0 = A_{FN} E_*^2 / [t^2(y)\phi_*], \; \phi_* = [(3.79\times10^{-4})^2 B_{FN}]^2,$$
$$E_* = 0.95 B_{FN} \phi_*^{3/2}, \; \tau_* = \frac{\pi m \sigma_{CE} B_p}{8ek} \left\{ \frac{A_{FN}}{\epsilon_o A_p t^2(y)[(3.79\times10^{-4})^2 B_{FN}]^2} \right\}^2$$

Coupling dimensionless variables and scaling terms with base breakdown equation yields dimensionless breakdown equation:

$$\frac{\exp[\bar{\phi}^{3/2}/(\beta\bar{E})]}{\beta\bar{\phi}^{1/2}\exp(\bar{\phi}^{-1/2})} \sqrt{\frac{\bar{\tau}\bar{E}}{\bar{p}\bar{d}^2}} \frac{\{1 - \gamma_{SE}[\exp(\bar{\alpha}\bar{d}) - 1]\}}{\exp(\bar{\alpha}\bar{d}) - 1} = \frac{\exp(x_o)(1 + 2\bar{E}x_o)}{x_o}$$

Gas	p_* ($\times 10^8$ Torr)	L ($\times 10^{-12}$m)	j_0 ($\times 10^{-18}$ A/m²)	ϕ_* (eV)	E_* ($\times 10^{12}$ V/m)	τ_* (K)
Argon	3.44	2.42	2.24	96.81	6.20	8476
Nitrogen	1.81	4.60	2.24	96.81	6.20	11288
Neon	6.20	4.03	2.24	96.81	6.20	21409
Xenon	1.77	2.17	2.24	96.81	6.20	11539

A. M. Loveless and A. L. Garner, *Phys. Plasmas* **24**, 113522 (2017).

Results

(1) Universal breakdown equation	$\frac{\exp[\bar{\phi}^{3/2}/(\beta\bar{E})]}{\beta\bar{\phi}^{1/2}\exp(\bar{\phi}^{-1/2})}\sqrt{\frac{\bar{\tau}\bar{E}}{\bar{p}\bar{d}^2}}\frac{\{1-\gamma_{SE}[\exp(\bar{\alpha}\bar{d})-1]\}}{\exp(\bar{\alpha}\bar{d})-1} = \frac{\exp(x_o)(1+2\bar{E}x_o)}{x_o}$
(2) Analytic solution with $\bar{\alpha}\bar{d} \ll 1$	$\bar{V} = \bar{d}\left[\frac{-\Delta_1-\sqrt{\Delta_1^2-2\Lambda_1(\bar{\phi}^{3/2}/\beta+\gamma_{SE}\bar{p}^2\bar{d}+\bar{p})}}{\Lambda_1}\right]$
(3) Analytic solution with $\bar{\alpha}\bar{d} \gg 1$	$\bar{V} = \bar{d}\left[\frac{-\Delta_2-\sqrt{\Delta_2^2-2\Lambda_2\bar{\phi}^{3/2}/\beta}}{\Lambda_2}\right]$
(4) Dimensionless Paschen's law	$\bar{V} = \frac{\bar{p}\bar{d}}{\ln[\bar{p}\bar{d}]-\ln[\ln(1+\gamma_{SE}^{-1})]}$

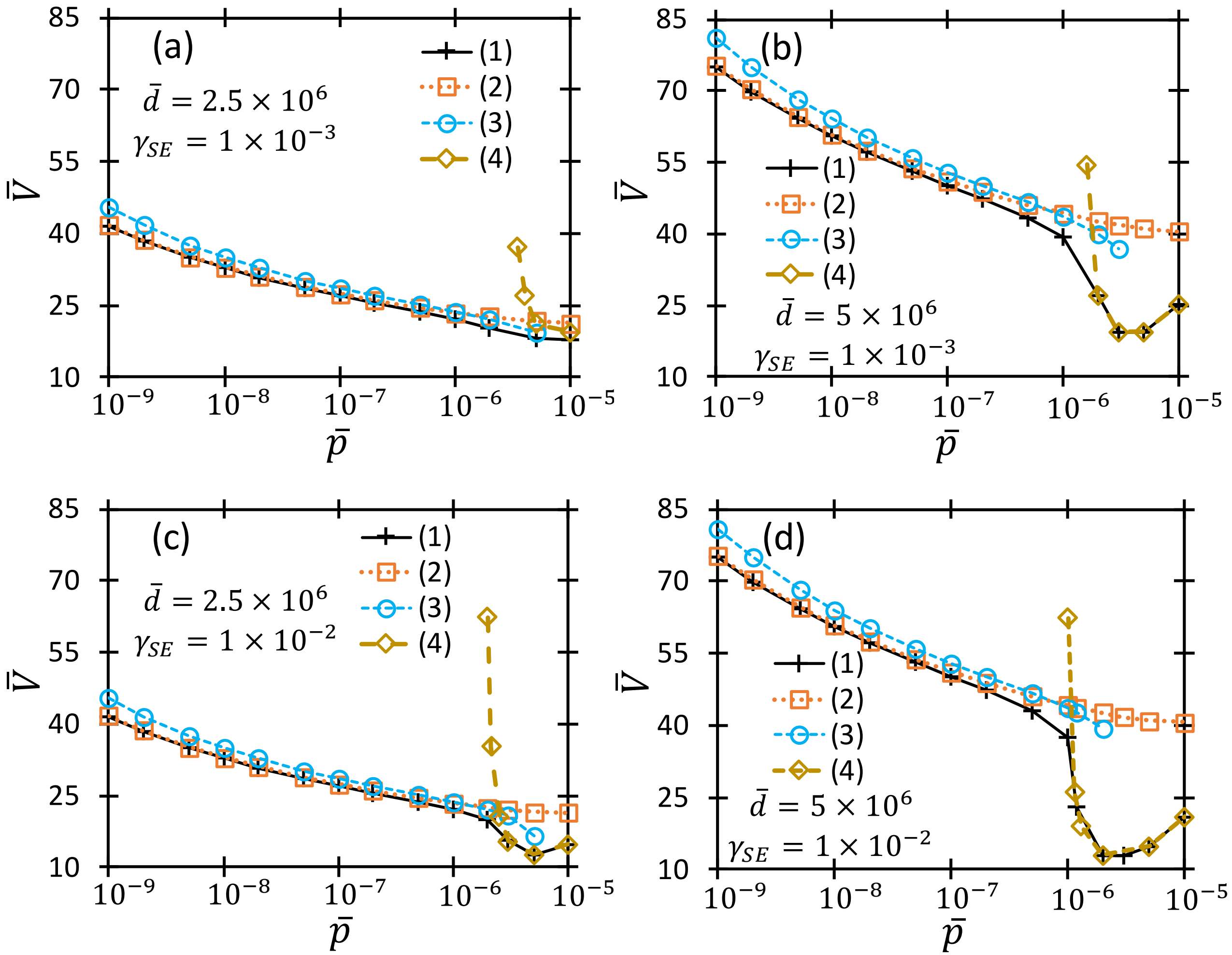

A. M. Loveless and A. L. Garner, *Phys. Plasmas* **24**,113522 (2017).

PURDUE UNIVERSITY School of Nuclear Engineering

Modeling Transition in Breakdown

Incorporate mean free path correction to ionization coefficient, given by

$\delta = 1 - \exp\left\{-\left[\left(\bar{d}/\bar{\lambda} - 1\right)/3.1\right]^{0.8}\right\}$

Split field emission and avalanche components of breakdown

$$\bar{V} = \frac{\bar{d}}{\Lambda_1}\left[-\Delta_1 - \sqrt{\Delta_1^2 - 2\Lambda_1\left(\frac{\bar{\phi}^{3/2}}{\beta} + \gamma_{SE}\bar{p}^2\bar{d}\delta + \bar{p}\right)}\right]$$

$$\Delta_1 = -\left[\ln\left(\beta\bar{\phi}^{1/2}\right) + \bar{\phi}^{-1/2} + \frac{\ln(\Lambda_1)}{2} + \ln\left(\bar{p}\bar{d}\delta\right) + \gamma_{SE}\bar{p}\bar{d} + \frac{3}{2} - \frac{\ln\left[\bar{T}/\left(\bar{p}\bar{d}^2\right)\right]}{2}\right]$$

$$\Delta_1 = [\tilde{\mu} + \tilde{\nu}]$$

$$\tilde{\mu} = \frac{\ln(\Lambda_1)}{2} + \ln\left(\beta\bar{\phi}^{1/2}\right) + \bar{\phi}^{-1/2} + \frac{3}{2}$$

Field emission

$$\tilde{\nu} = \ln\left(\bar{p}\bar{d}\right) + \gamma_{SE}\bar{p}\bar{d} - \frac{\ln\left[\bar{\tau}/\left(\bar{p}\bar{d}^2\right)\right]}{2}$$

Townsend avalanche

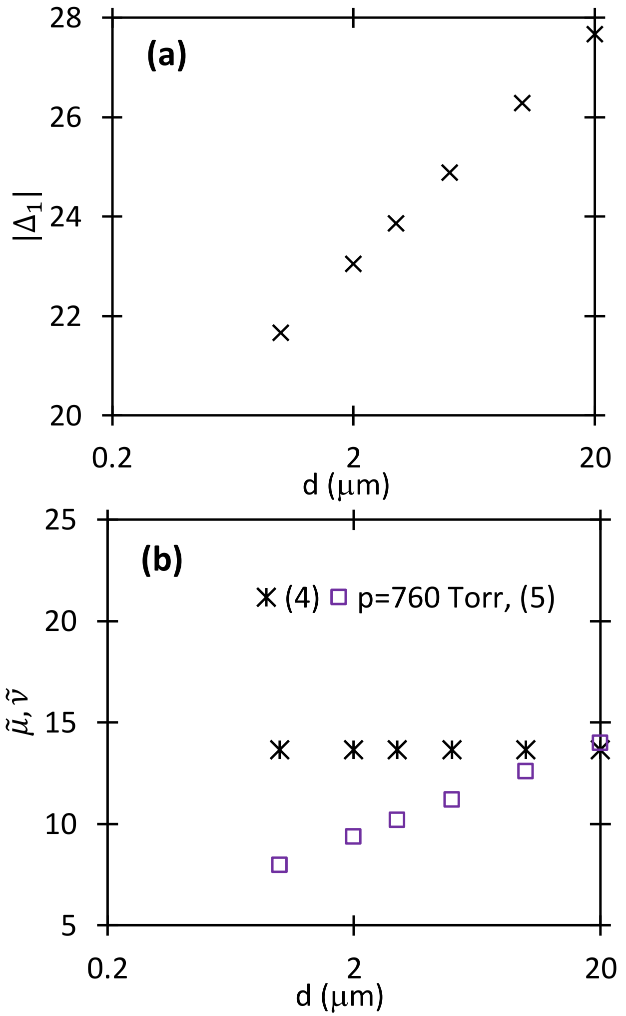

G. Meng, X. Gao, A. M. Loveless, C. Dong, D. Zhang, K. Wang, B. Zhu, Y. Cheng, and A. L. Garner, *Phys. Plasmas* **25**, 082116 (2018).

Comparing Theory to Experiment

For field emission, we obtain

$$\bar{V} = \frac{\bar{d}}{\Delta_1}\left(\frac{\bar{\phi}^{3/2}}{\beta} + \gamma_{SE}\bar{p}^2\bar{d}\delta + \bar{p}\right) \approx \left(\frac{\bar{\phi}^{3/2}}{\beta\Delta_1}\right)\bar{d}$$

(a) = Experimental breakdown voltage and electric field
(b) = Measured breakdown voltage and theoretical

(1) = Exact Numerical solution
(8) = Simplified field emission equation above
(9) = Universal Paschen's law

β increases linearly in the field emission regime and begins to flatten as the breakdown mechanism transitions to Townsend avalanche

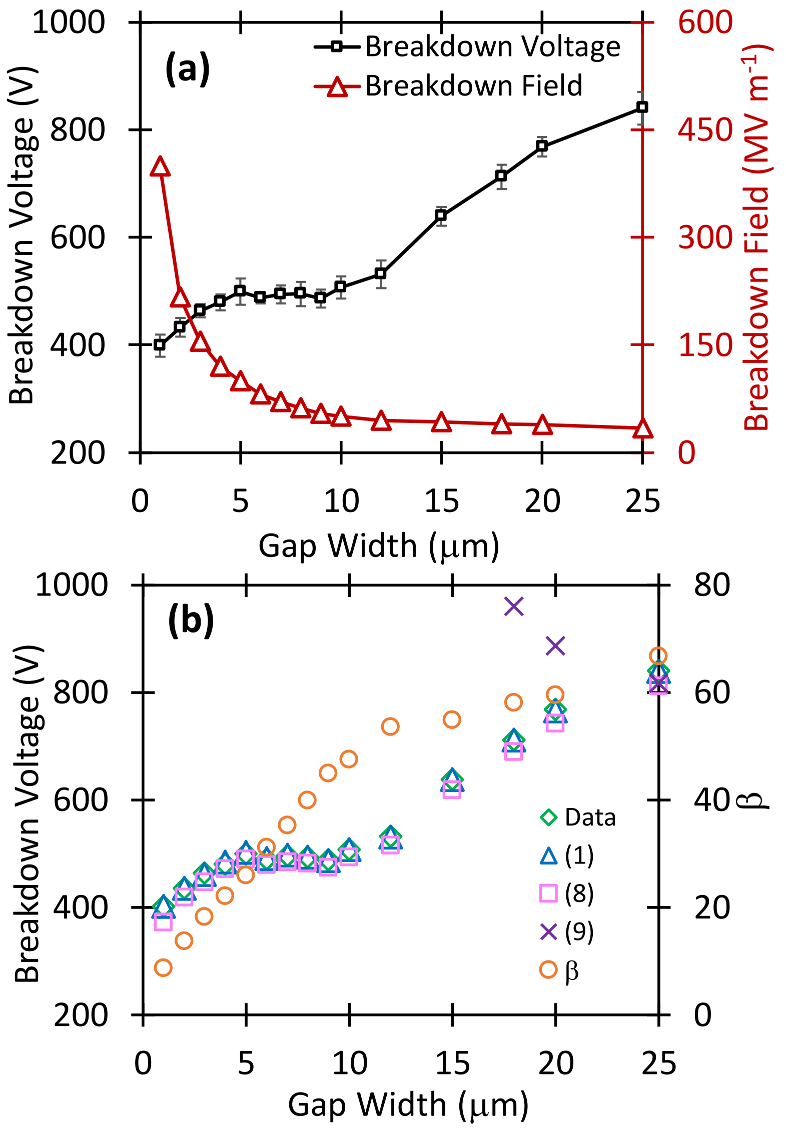

G. Meng, X. Gao, A. M. Loveless, C. Dong, D. Zhang, K. Wang, B. Zhu, Y. Cheng, and A. L. Garner, *Phys. Plasmas* **25**, 082116 (2018).

Assess Scaling Using Universal Plots

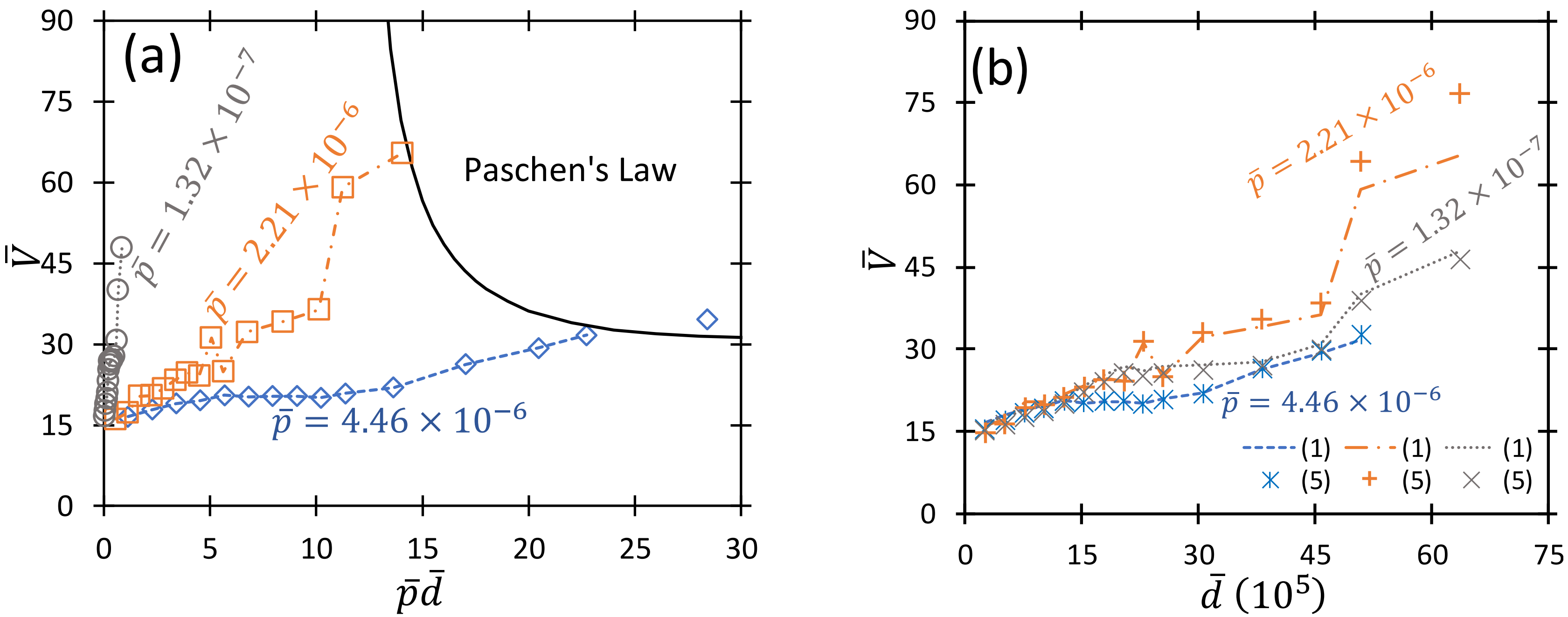

- Universal scaling with *pd* at high *pd* – **Paschen's law**
- Universal scaling with d at low *d* – **Field emission regime**

A. M. Loveless, G. Meng, Q. Ying, F. Wu, K. Wang, Y. Cheng, and A. L. Garner, Sci. Rep. **9**, 5669 (2019).

Surface Roughness Effect on Work Function

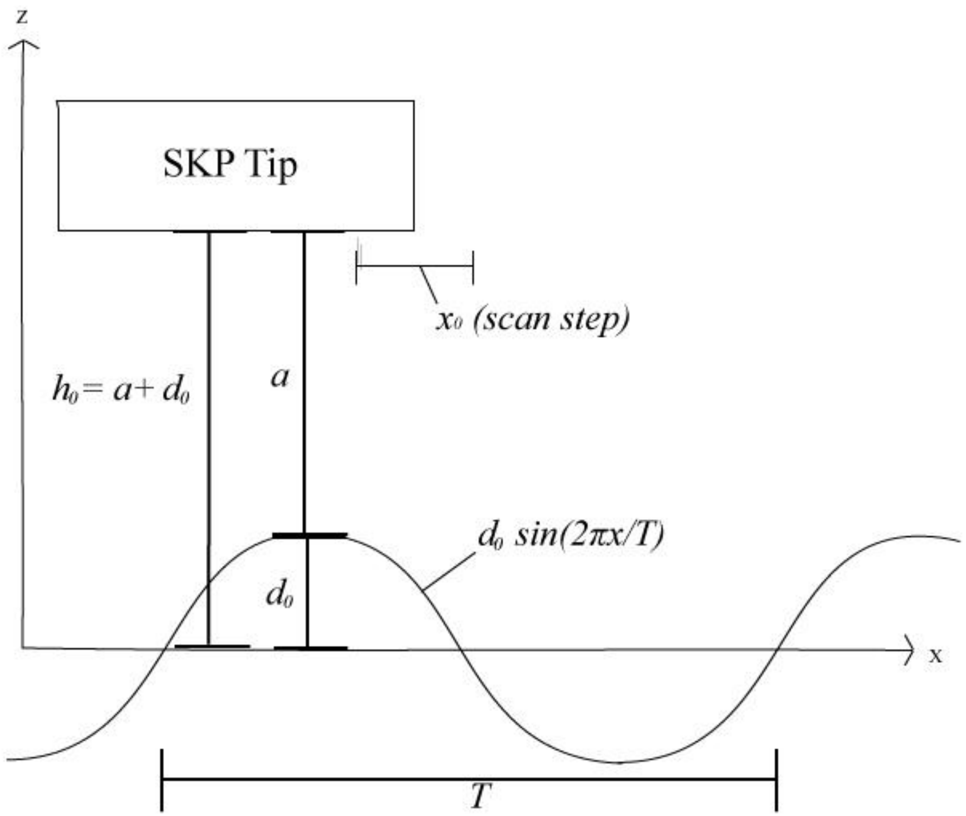

Visualization of the parameters when using a scanning Kelvin probe to measure the work function of a rough surface.

Past studies neglect this

Surface Roughness Model $$z(x) = d_0 \sin\left(\frac{2\pi x}{T}\right) \quad (1)$$

Surface Roughness δ $$\delta = \frac{d_0}{\sqrt{2}}. \quad (2)$$

Work function of a surface: $$\varphi_s = \varphi_t - \frac{eQ}{C_k}, \quad (3)$$

Equation for capacitance: $$C_k = \int dC_k = \int_{nx_0}^{(n+1)x_0} \frac{\varepsilon_0 y_0 dx}{h_0 - d_0 \sin\left(\frac{2\pi x}{T}\right)} = \varepsilon_0 y_0 \int_{nx_0}^{(n+1)x_0} \frac{dx}{h_0 - d_0 \sin\left(\frac{2\pi x}{T}\right)} \quad (4)$$

Charge per SKP scan step: $$Q = \frac{Q'S}{A} = \frac{\varepsilon_0 x_0 y_0 (\varphi_t^0 - \varphi_s^0)}{ea} \quad (5)$$

Y. Wan, et al., J. Electrochem. Sci. **7**, 5204-5216 (2012).

Substitute (4) and (5) into (3), yielding effective work function of surface:

$$\varphi_s = {\varphi_t}^0 - \frac{x_0(\varphi_t^0 - \varphi_s^0)}{a} \frac{\pi}{T} \left(\frac{1}{m}\right) \sqrt{h_0^2 - d_0^2} \sum_{n=1}^{n=m} \left(\frac{1}{\arctan\left(\frac{d_0 + h_0 \tan\left(\frac{\pi}{T}(n)x_0\right)}{\sqrt{h_0^2 - d_0^2}}\right) - \arctan\left(\frac{d_0 + h_0 \tan\left(\frac{\pi}{T}(n-1)x_0\right)}{\sqrt{h_0^2 - d_0^2}}\right)} \right)$$

PURDUE UNIVERSITY | School of Nuclear Engineering

J. R. Malayter and A. L. Garner, AIP Adv. **10**, 095110 (2020).

Surface Roughness Effect on Work Function

Nondimensionalized model for effective work function of a rough surface:

$$\overline{\varphi_s} = \overline{\varphi_t{}^0} - \frac{\overline{(\varphi_t{}^0)}-1}{a}\frac{\pi}{\tau}\sqrt{h_0^2-d_0^2}\left(\frac{1}{m}\right)\sum_{n=1}^{n=m}\left(\frac{1}{\arctan\left(\frac{d_0+h_0\tan\left(\frac{\pi}{\tau}(n)\right)}{\sqrt{h_0^2-d_0^2}}\right)-\arctan\left(\frac{d_0+h_0\tan\left(\frac{\pi}{\tau}(n-1)\right)}{\sqrt{h_0^2-d_0^2}}\right)}\right) \quad (7)$$

where: $\overline{\varphi_s} = \frac{\varphi_s}{\varphi_s^0}$, $\overline{\varphi_t{}^0} = \frac{\varphi_t^0}{\varphi_s^0}$, and $\tau = \frac{T}{x_0}$

Taking the limit of the model as $\tau \to \infty$ using L'Hôpital's rule and the small angle theory:

$$\overline{\varphi_{s,Ave}} = \overline{\varphi_t^0} - \frac{\left(\overline{\varphi_t^0}-1\right)}{a}h_0 \quad (8)$$

Limit for $d_0/h_0 \ll 1$ (Taylor series approximation):

$$\overline{\varphi_{s,Ave}} = 1 - \frac{d_0}{h_0}\left(\overline{\varphi_t^0}-1\right) \quad (9)$$

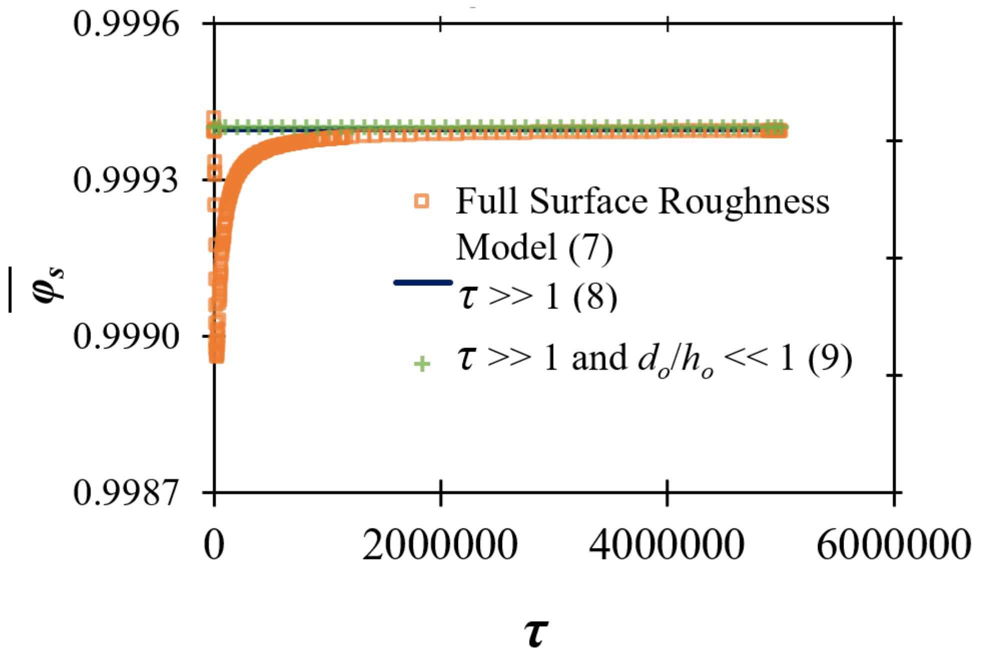

J. R. Malayter and A. L. Garner, AIP Adv. **10**, 095110 (2020).

Experimental Setup

- Tungsten dissection needles
    - 1 µm tip (Roboz Surgical Instrument Co., RS-6
- Copper plate cut to 12.7 mm^2
- Two 1 MΩ resistors
    - Current limiting
    - Current viewing shunt
- DC high voltage supply (Stanford Research System, kV)
- Two 100:1 voltage probes were connected across pin-plate connection and shunt resistor
- LeCroy Oscilloscope to record voltage and current at breakdown

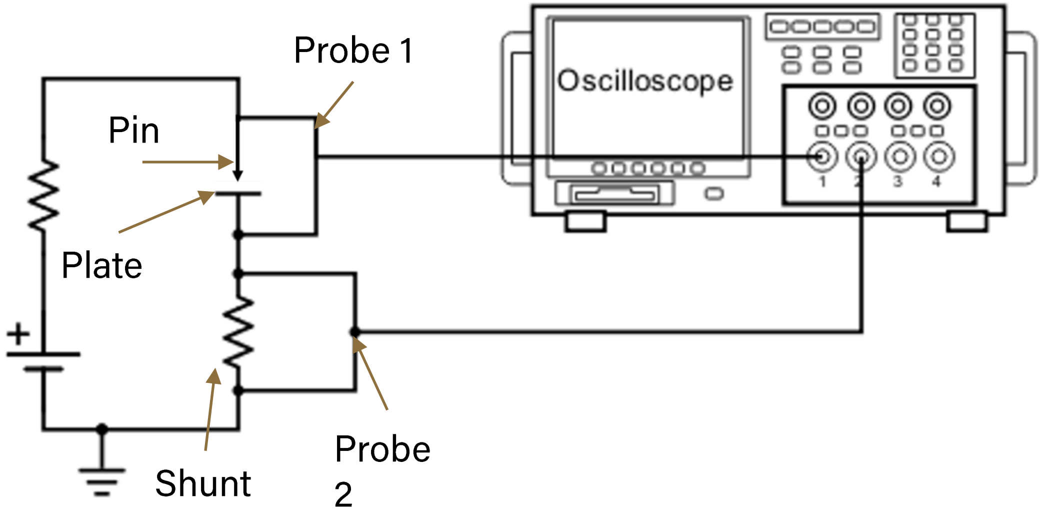

R. S. Brayfield, II, A. J. Fairbanks, A. M. Loveless, S. Gao, A. Dhanabal, W. Li, C. Darr, W. Wu, and A. L. Garner, J. Appl. Phys. **125**, 203302 (2019).

Experimental Design

- Copper plate surface modification
  - Wet polishing station with 400, 800, and 1200 grit polishing pads (Pace Technologies)
  - After polish the samples were soaked in acetone
- Plate surface divided into 2 regions
  - 1 breakdown event
  - 10 breakdown events
- AFM conducted pre-test
  - Initial surface roughness
  - Contamination
- Gaps distance set
  - Applied 35 V and shorted gap
  - 1, 5, and 10 µm
- Voltage slowly increased (~3V/s) until breakdown occurred
  - Current across gap observed on oscilloscope
- Measure voltage and current at which gap broke down

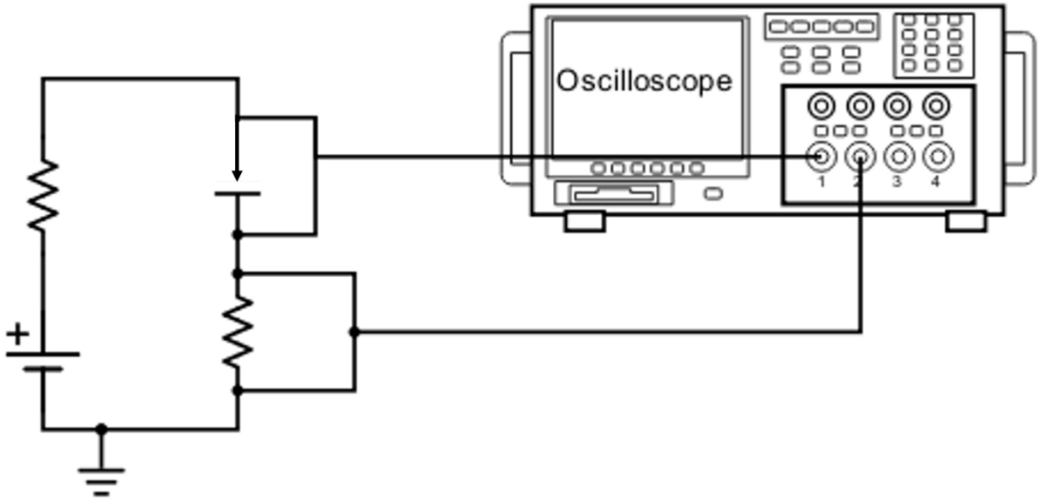

R. S. Brayfield, II, A. J. Fairbanks, A. M. Loveless, S. Gao, A. Dhanabal, W. Li, C. Darr, W. Wu, and A. L. Garner, J. Appl. Phys. **125**, 203302 (2019).

Surface Roughness and Craters

Grit	Number of samples	Peak to Peak Average (μm)	Standard Deviation (μm)	RMS (nm)
400	9	1.47	1.08	535.22
800	9	0.26	0.18	65.99
1200	9	0.24	0.23	39.48

- Considered the impact of three different surface roughnesses.
- At the smaller gap distances and greater surface roughness, several samples exhibited craters on the order of (and often larger) than the gap interelectrode gap distance.

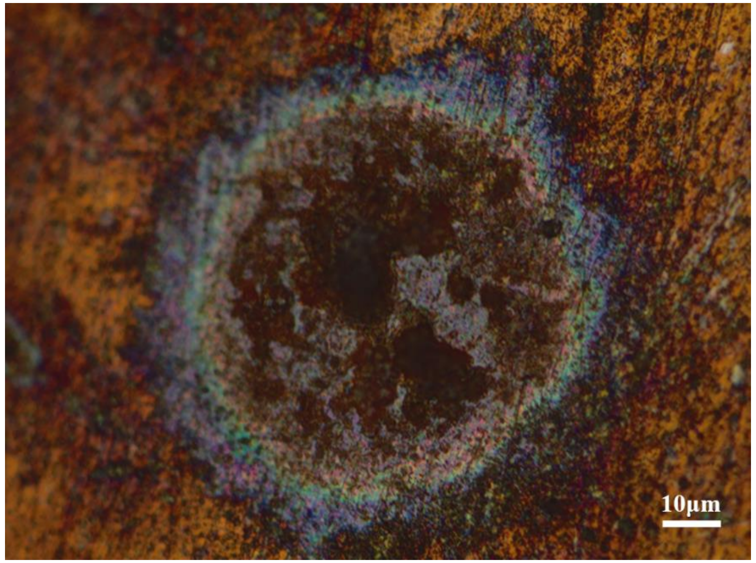

Grit (gap distance)	Depth (μm)	Grit (gap distance)	Depth (μm)	Grit (gap distance)	Depth (μm)
400 (10 μm)	9.7	800 (5 μm)	6.2	1200 (1 μm)	12.1
400 (10 μm)	6	800 (5 μm)	7.4	1200 (1 μm)	3.5
400 (10 μm)	13.5	800 (5 μm)	12.4	1200 (10 μm)	4.8
400 (5 μm)	41.2	800 (5 μm)	5.3	1200 (10 μm)	5.4
400 (5 μm)	19.6	800 (5 μm)	5.2		
400 (1 μm)	42.5				

R. S. Brayfield, II, A. J. Fairbanks, A. M. Loveless, S. Gao, A. Dhanabal, W. Li, C. Darr, W. Wu, and A. L. Garner, J. Appl. Phys. **125**, 203302 (2019).

Results: Altered Breakdown Voltage

Larger gap did not always result in higher breakdown voltage

Crater significantly impacted required breakdown voltage

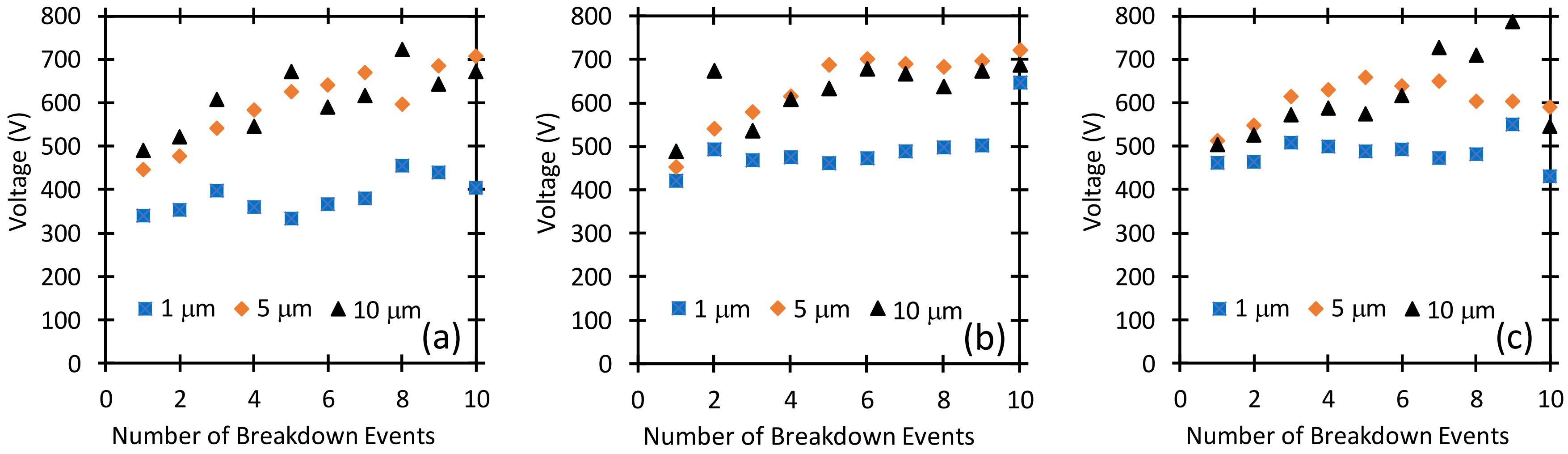

(a) 400 grit
(b) 800 grit
(c) 1200 grit

- Larger gap did not always result in higher breakdown voltage
- Crater significantly impacted required breakdown voltage

R. S. Brayfield, II, A. J. Fairbanks, A. M. Loveless, S. Gao, A. Dhanabal, W. Li, C. Darr, W. Wu, and A. L. Garner, J. Appl. Phys. **125**, 203302 (2019).

Results: Data vs. Model

- (1): Numerical solution
- (2): Analytic solution
- (1) and (2) differ by ~10% until the largest gap distances
- At largest gap distances, $\bar{\alpha}\bar{d}_{eff} > 18$ – Meek's criterion for streamer discharge

Can we get streamers at microscale?

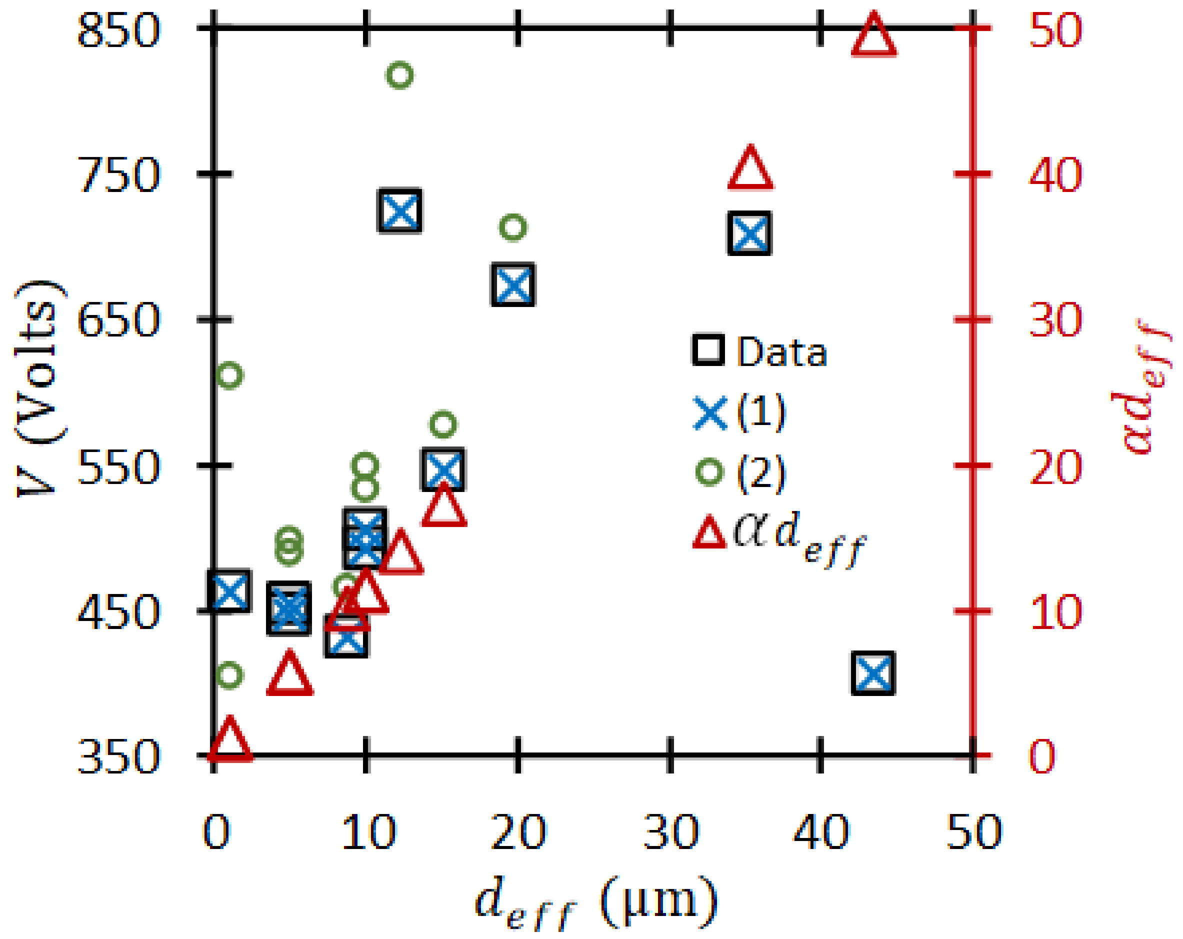

R. S. Brayfield, II, A. J. Fairbanks, A. M. Loveless, S. Gao, A. Dhanabal, W. Li, C. Darr, W. Wu, and A. L. Garner, J. Appl. Phys. **125**, 203302 (2019).

Conceptual Framework of Emission Mechanism Transitions

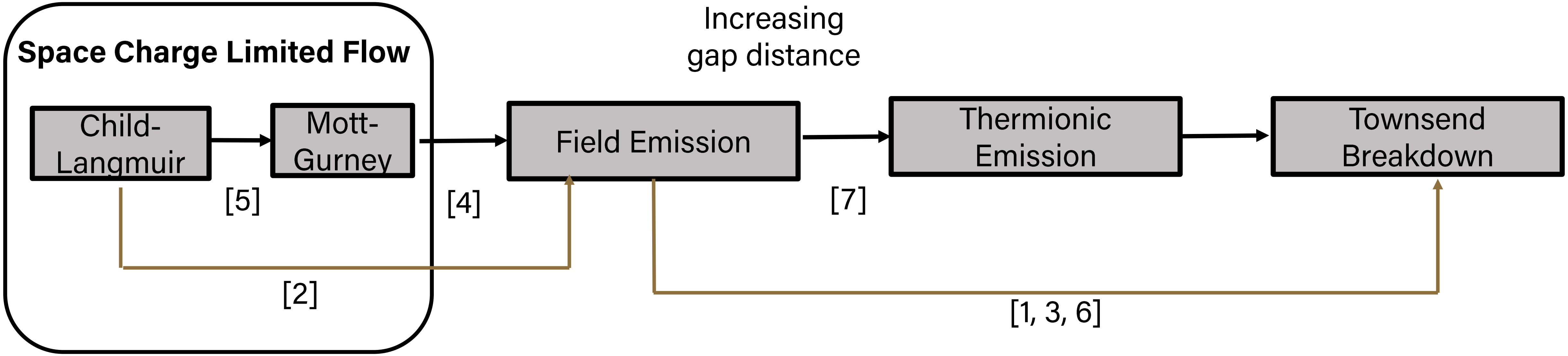

[1] A. Venkattraman and A. A. Alexeenko, Phys. Plasmas **19**, 123515 (2012).
[2] Y. Y. Lau, Y. Liu, and R. K. Parker, Phys. Plasmas **1**, 2082-2085 (1994).
[3] D. B. Go and D. A. Pohlman, J. Appl. Phys. **107**, 103303 (2010).
[4] A. M. Darr, A. M. Loveless, and A. L. Garner, Appl. Phys. Lett. **114**, 014103 (2019).
[5] M. S. Benilov, Plasma Sources Sci. Technol. **18**, 014005 (2009).
[6] A. L. Garner, A. M. Loveless, J. N. Dahal, and A. Venkattraman, IEEE Trans. Plasma Sci. **48**, 808-824 (2020).
[7] A. M. Darr, C. R. Darr, and A. L. Garner, Phys. Rev. Research **2**, 033137 (2020).
[8] M. U. Lee, J. Lee, J. K. Lee, and G. S. Yun, Plasma Sources Sci. Technol. **26**, 034003 (2017).

Nexus Theory – Connections of Emission Mechanisms

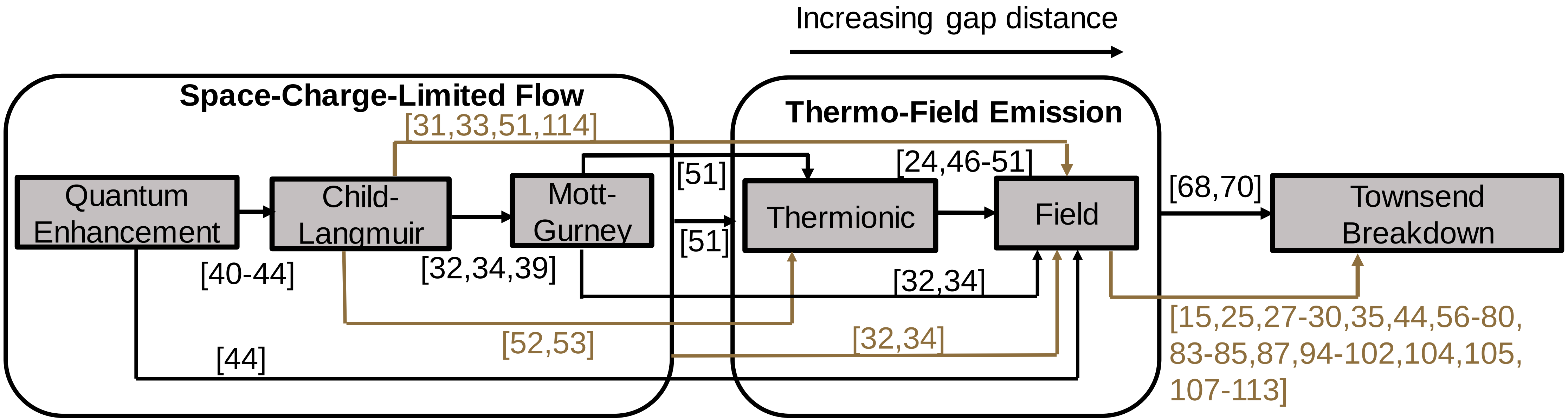

A. L. Garner, G. Meng, Y. Fu, A. M. Loveless, R. S. Brayfield, and A. M. Darr, J. Appl. Phys., Submitted.

Transitions Across Child-Langmuir, Mott-Gurney, and Fowler-Nordheim

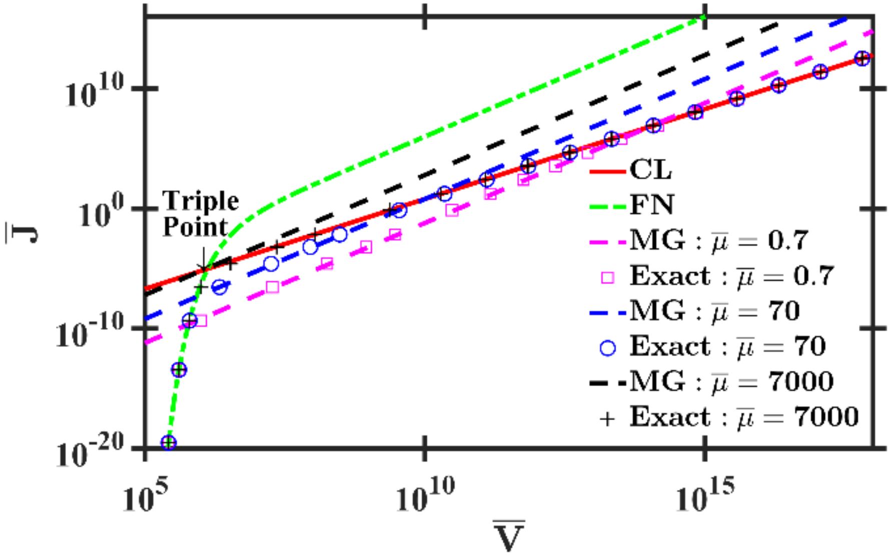

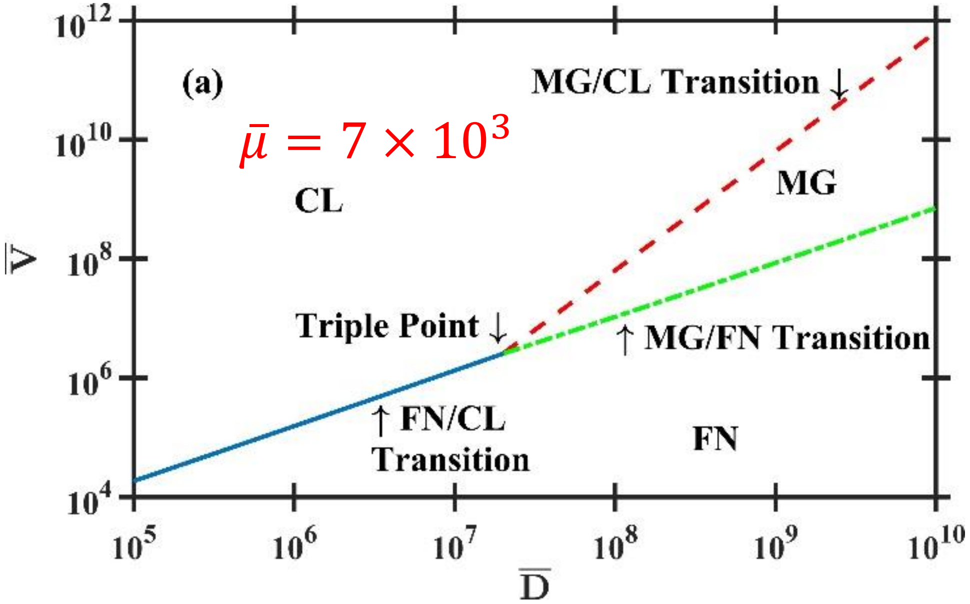

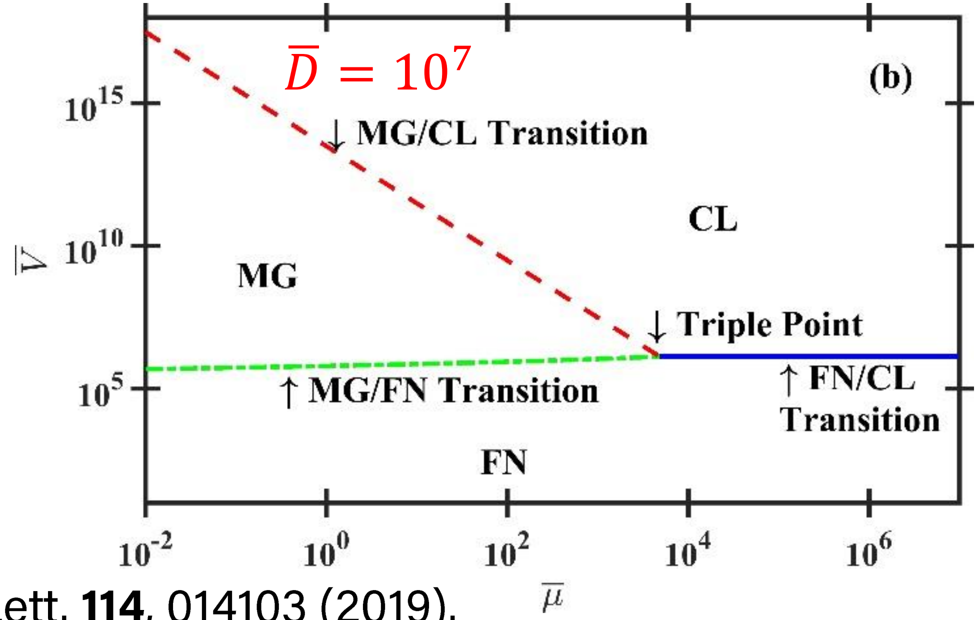

Below "triple point": FN → MG → CL

Above "triple point": FN → CL

$$\bar{J}_{CL} = \left(4\sqrt{2}/9\right)\bar{V}^{3/2}/\bar{D}^2$$

$$\bar{J}_{FN} = (\bar{V}^2/\bar{D}^2)e^{-\bar{D}/\bar{V}}$$

$$\bar{J}\bar{D}^2 = \frac{9\bar{V}^2\bar{\mu}}{8\bar{D}}$$

A. M. Darr, A. M. Loveless, and A. L. Garner, Appl. Phys. Lett. **114**, 014103 (2019).

Conditions for Third Order Nexus: FN = MG =C L

Triple point (third order nexus) occurs when FN = MG = CL

$$\bar{D} = \bar{V}\ln\left[\left(9\sqrt{\bar{V}}\right)/\left(4\sqrt{2}\right)\right]$$

$$\bar{\mu} = \left(32\sqrt{2\bar{V}}/81\right)\ln\left[\left(9\sqrt{\bar{V}}\right)/\left(4\sqrt{2}\right)\right]$$

Defining $\bar{D}, \bar{V}$, or $\bar{\mu}$ uniquely defines the other two parameters to achieve a third order nexus.

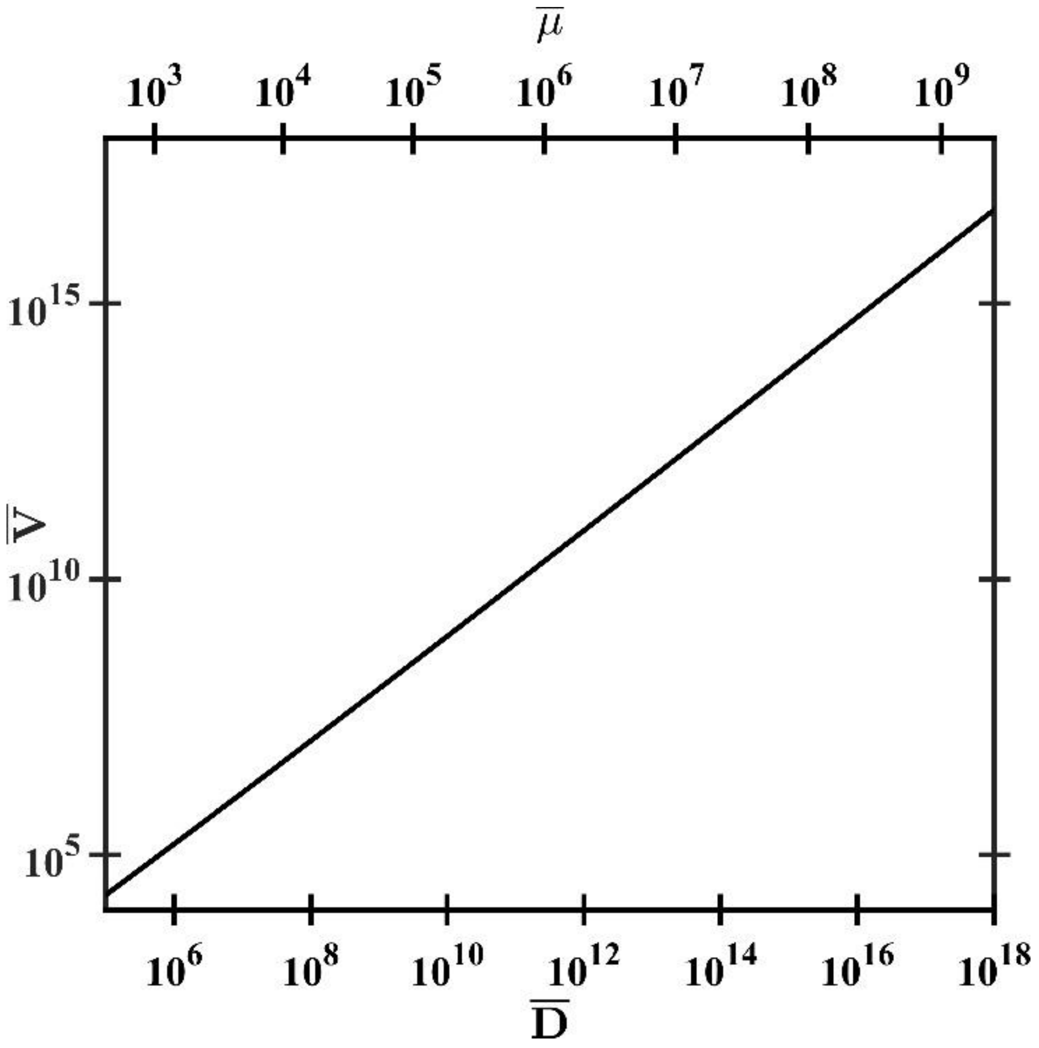

Examples: Pressure necessary for a triple point at 250 nm
Argon: 243 Torr
Nitrogen: 791 Torr

- ➔ At atmospheric pressure, the triple point for air is on the order of several hundred nm.
- ➔ Microscale gas breakdown is driven by field emission.
- ➔ For slightly smaller gaps, does SCLE contribute?

Nexus: Thermal/Field/Space-charge Limited Emission

FE + CL + MG (including pressure)

FE + TE: Thermo-field emission

FE + CL: Miram curve

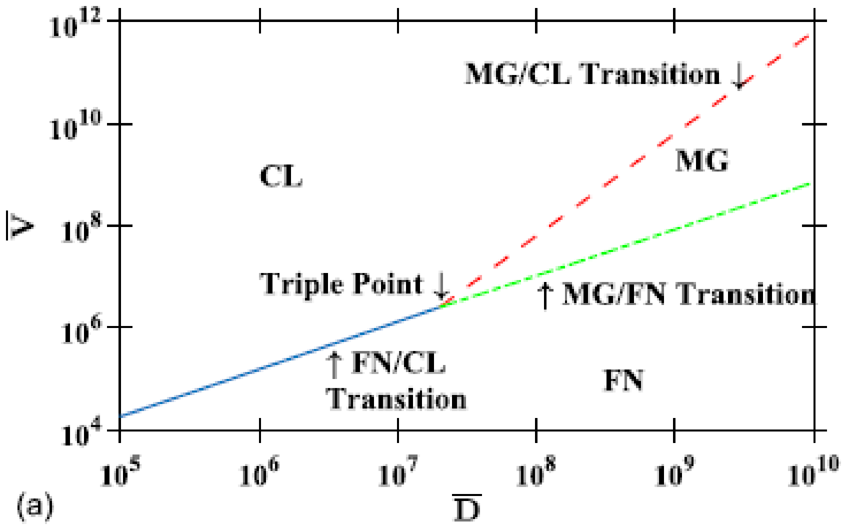

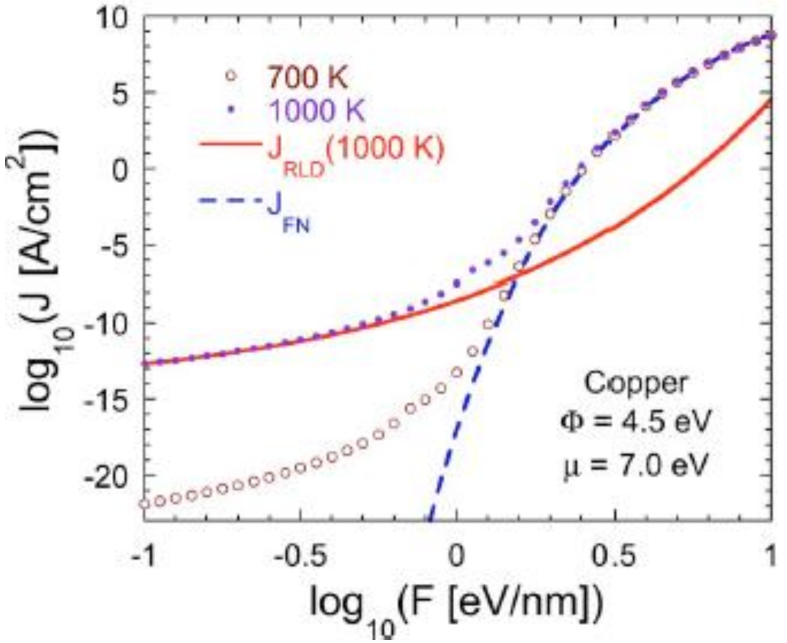

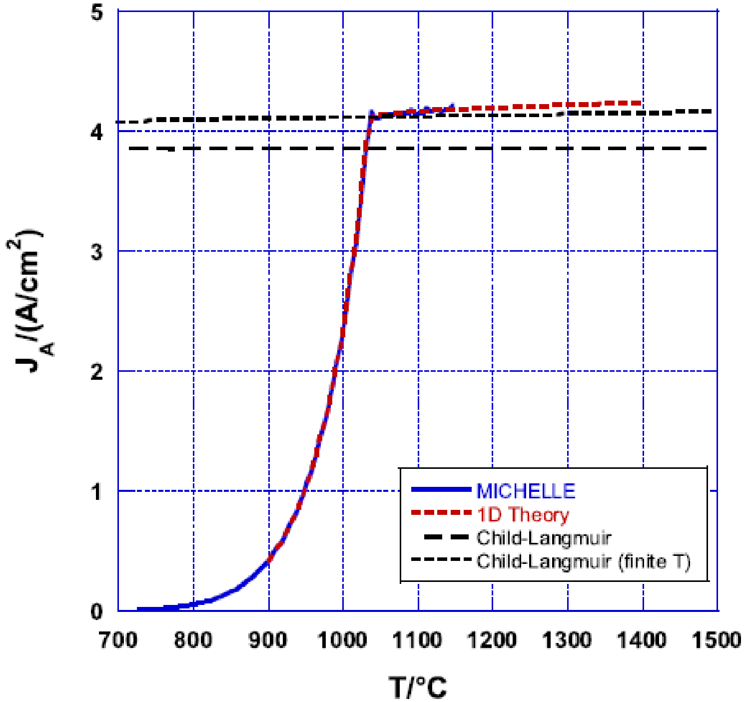

[1] A. M. Darr, A. M. Loveless, and A. L. Garner, Appl. Phys. Lett. **114**, 014103 (2019); [2] K. L. Jensen, *J. Appl. Phys.* **102**, 024911 (2007); [3] D. Chernin, Y. Y. Lau, J. J. Petillo, et al., IEEE Trans. Plasma Sci. **48**, 146-155 (2020).

Current/Voltage for $\bar{D} = 0.55$

(a) $\bar{T}=0.03\bar{T}_N$, (b) $0.15\bar{T}_N$, and (c) $\bar{T}_N$,
$\bar{T}_N = 1.98 \equiv$ nexus between FN, RLD, and CL.

$$\bar{J}_{CL} = \left(4\sqrt{2}/9\right)\bar{V}^{3/2}/\bar{D}^2$$

$$\bar{J}_{FN} = (\bar{V}^2/\bar{D}^2)e^{-\bar{D}/\bar{V}}$$

$$\bar{J}_{RLD} = \frac{9}{4}\bar{T}^2 e^{-1/\bar{T}},$$

$$\bar{J}_{GCL} \approx \bar{J}_{CL}\left(1 + 3\sqrt{\frac{\bar{v}_i^2}{2\bar{V}}}\right),$$

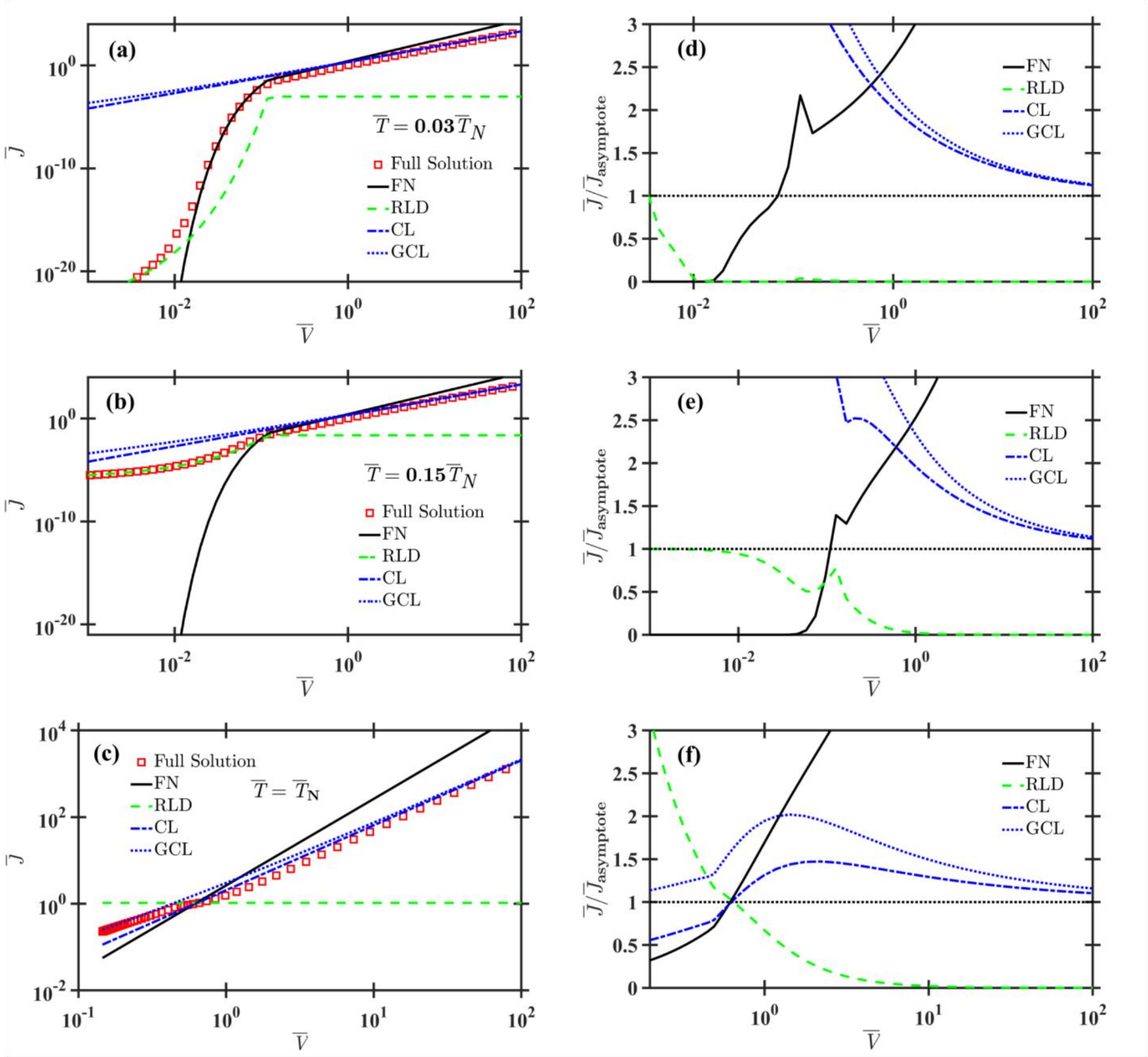

PURDUE UNIVERSITY | School of Nuclear Engineering

A. M. Darr, C. R. Darr, and A. L. Garner, Phys. Rev. Research **2**, 033137 (2020).

Field Enhanced Miram Curve at $\bar{D} = 0.55$

The standard Miram curve gradually transitions to unity at high $\bar{T}$.

A field contribution at high dimensionless voltage $\bar{V}$ gives a baseline current contribution and softens the knee where the behavior transitions to space-charge.

(a) Traditional Miram curve.

(b) Slight field enhancement at low temperatures.

(c) The nexus $\bar{V}$ causes significant field emission and a soft knee at transition to GCL.

(d) Near-space-charge levels of field contribution leading to a higher temperature transition to SCLE.

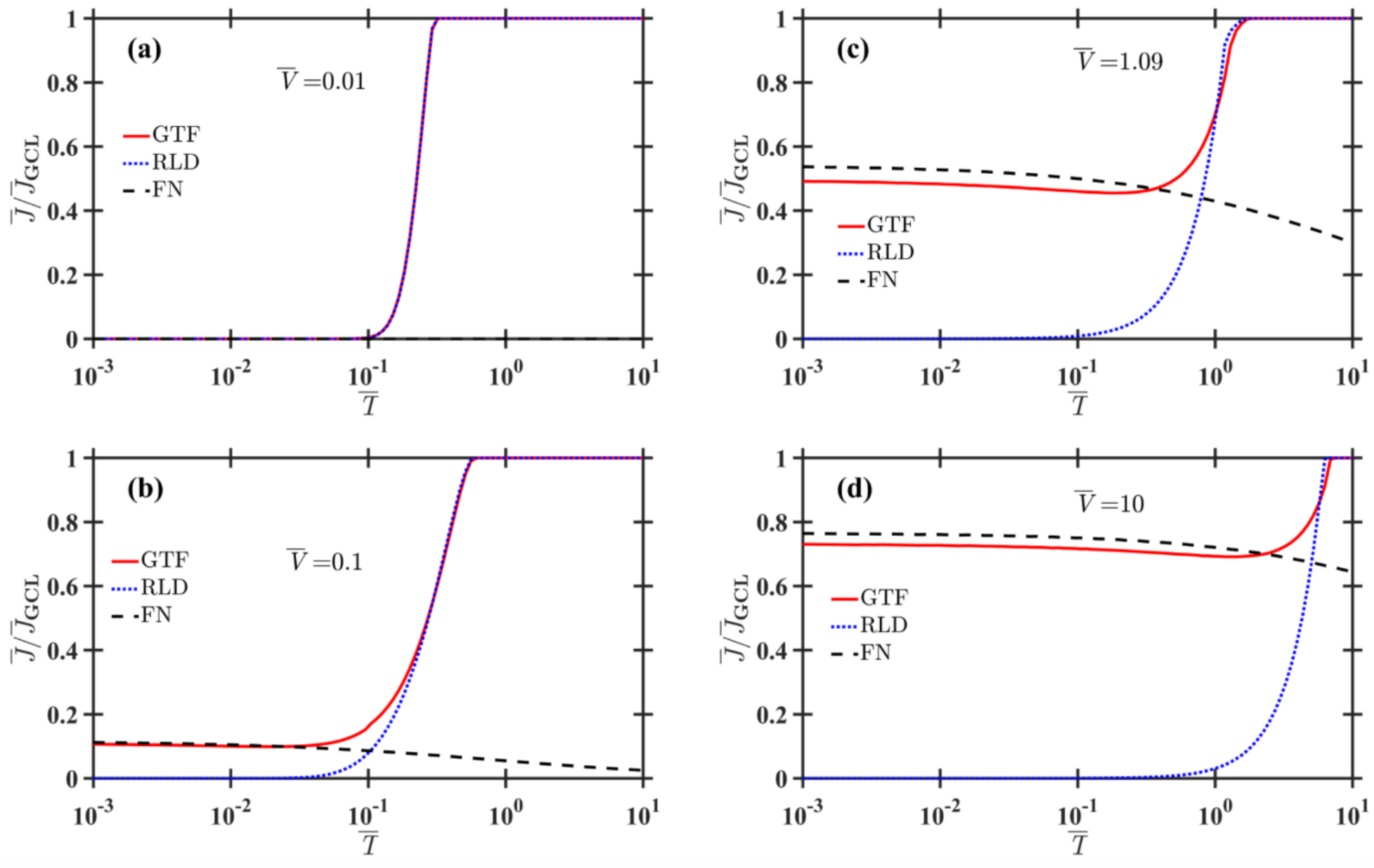

A. M. Darr, C. R. Darr, and A. L. Garner, Phys. Rev. Research **2**, 033137 (2020).

May Construct Nexuses for Any Condition

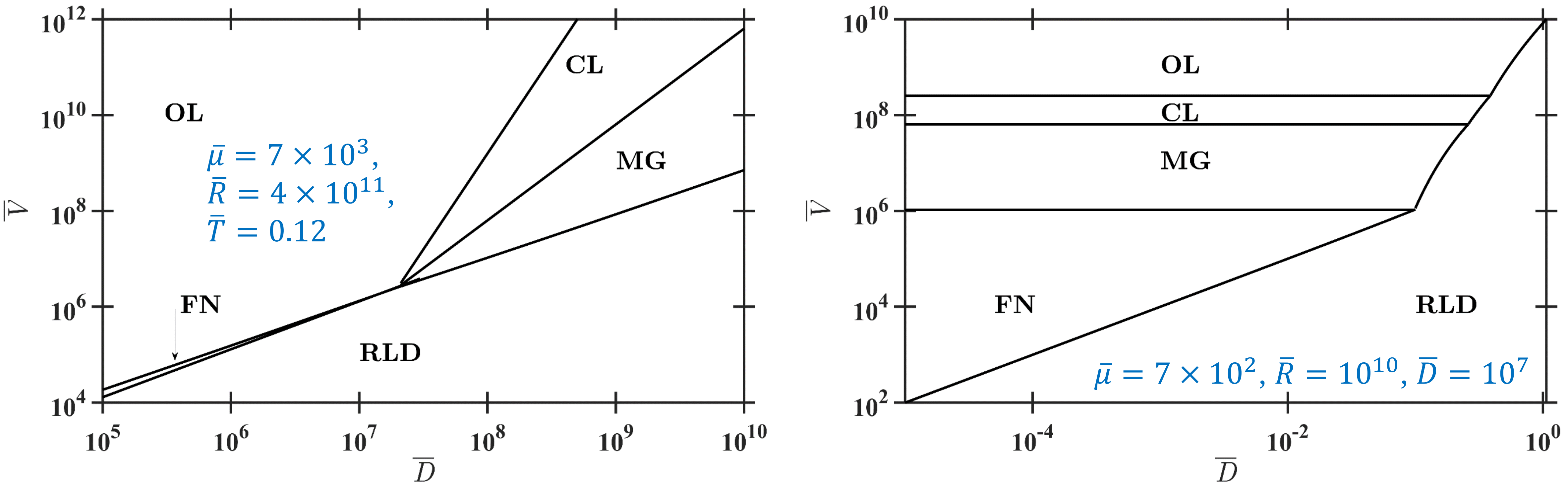

PURDUE UNIVERSITY | School of Nuclear Engineering

A. M. Darr, C. R. Darr, and A. L. Garner, Phys. Rev. Research **2**, 033137 (2020).

Nanoscale Emission and Breakdown at Atmospheric Pressure

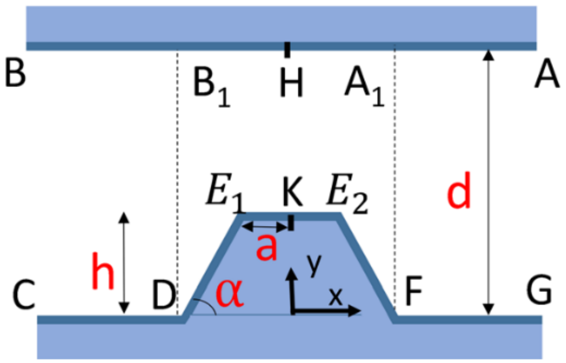

Geometry from: J. Lin, P. Y. Wong, P. Yang, Y. Y. Lau, W. Tang, and P. Zhang, J. Appl. Phys. **121**, 244301 (2017).

a = 38 nm
h = 769 nm
d = 1000 nm
$d - h$ = 231 nm

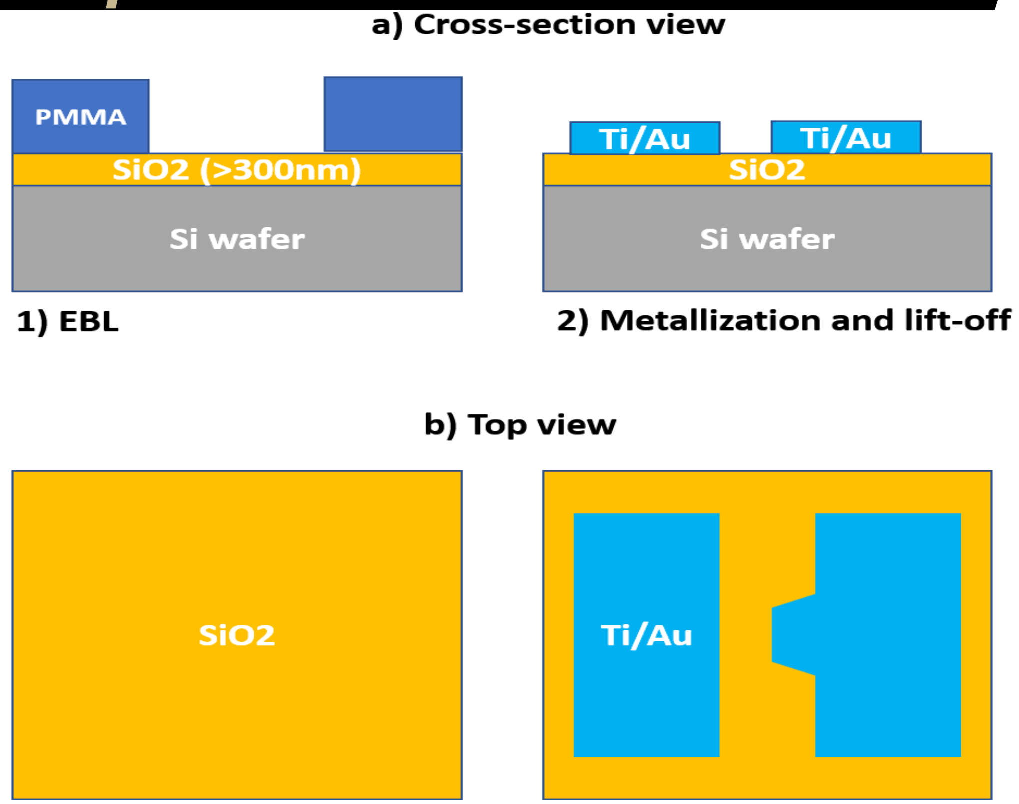

Device fabrication layout showing layers of material used in process

Fabricated multiple combinations of *a*, *h*, and *d*

Experiments at d_{eff}= 28 ± 10 nm at Atmospheric Pressure

Emission area = 64 nm^2

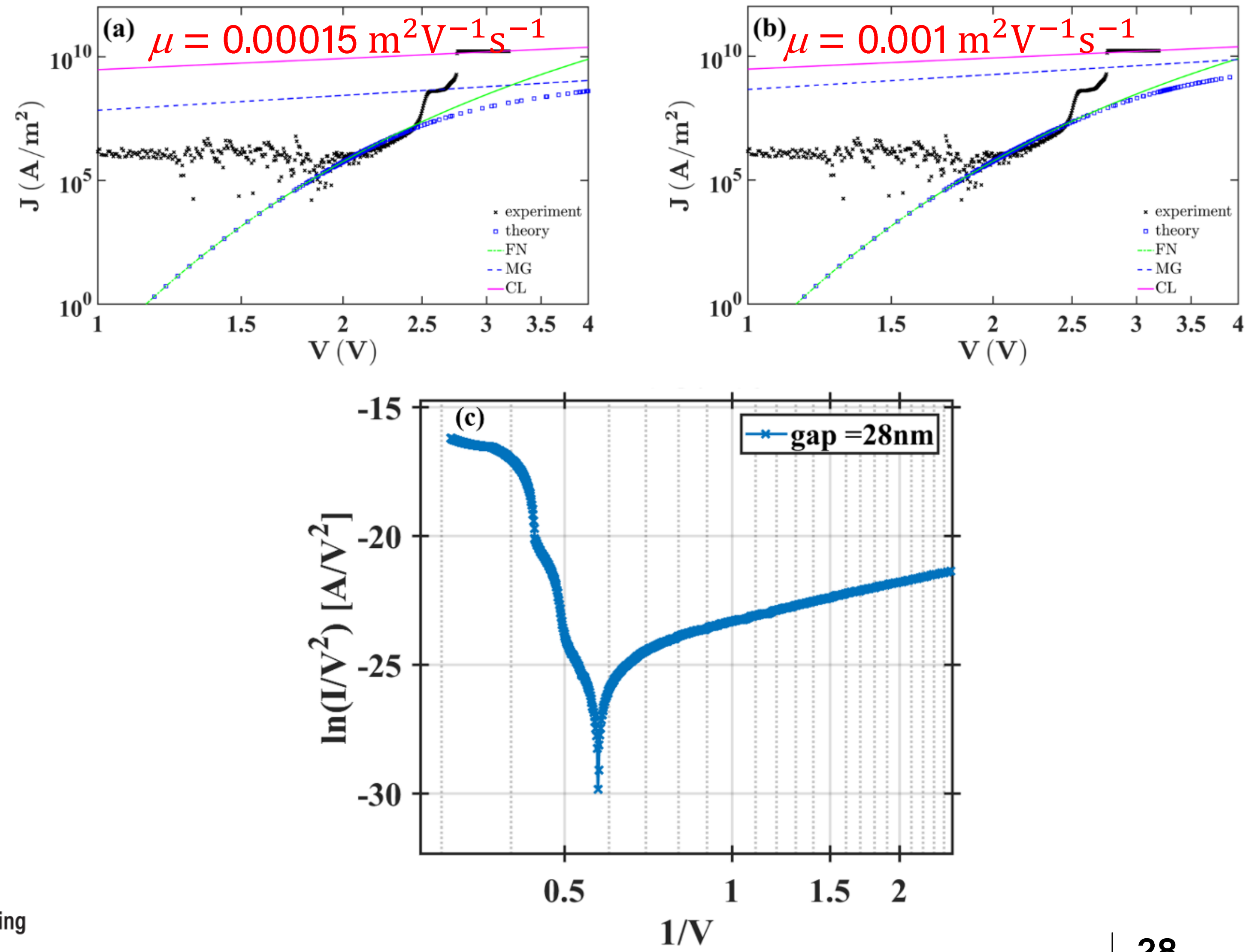

Transitions from FN to breakdown.

PURDUE UNIVERSITY | School of Nuclear Engineering

Experiments at $d_{eff} = 125 \pm 10$ nm at Atmospheric Pressure

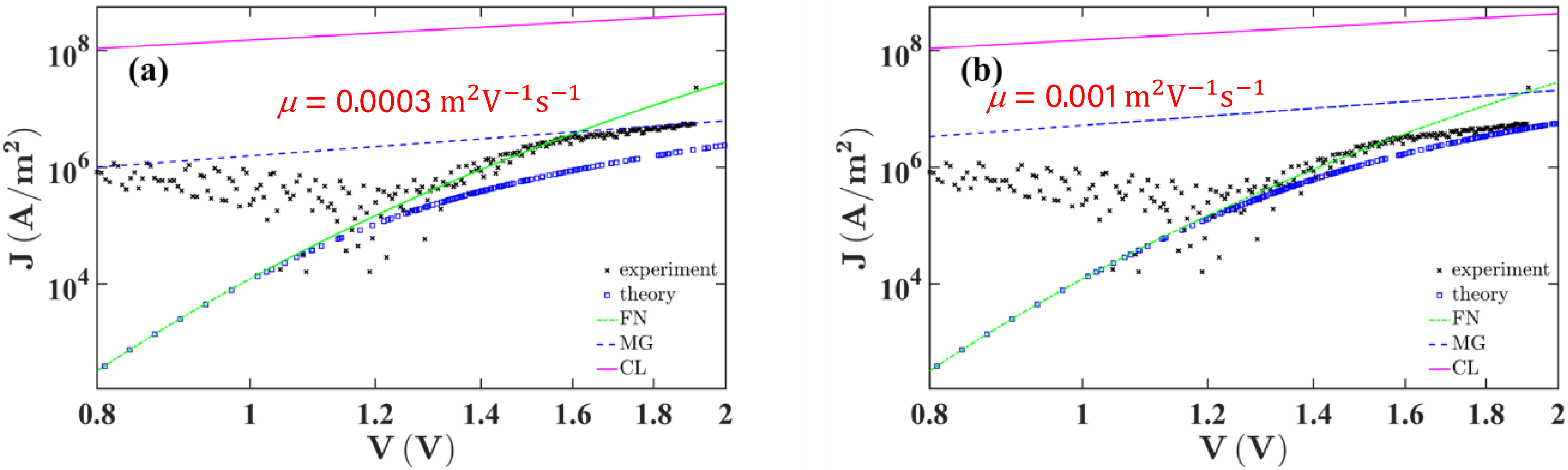

High μ better predicts the overall behavior of the experimental data.

Experiments at d_{eff} = 450 ± 10 nm at Atmospheric Pressure

Emission area = 64 nm^2

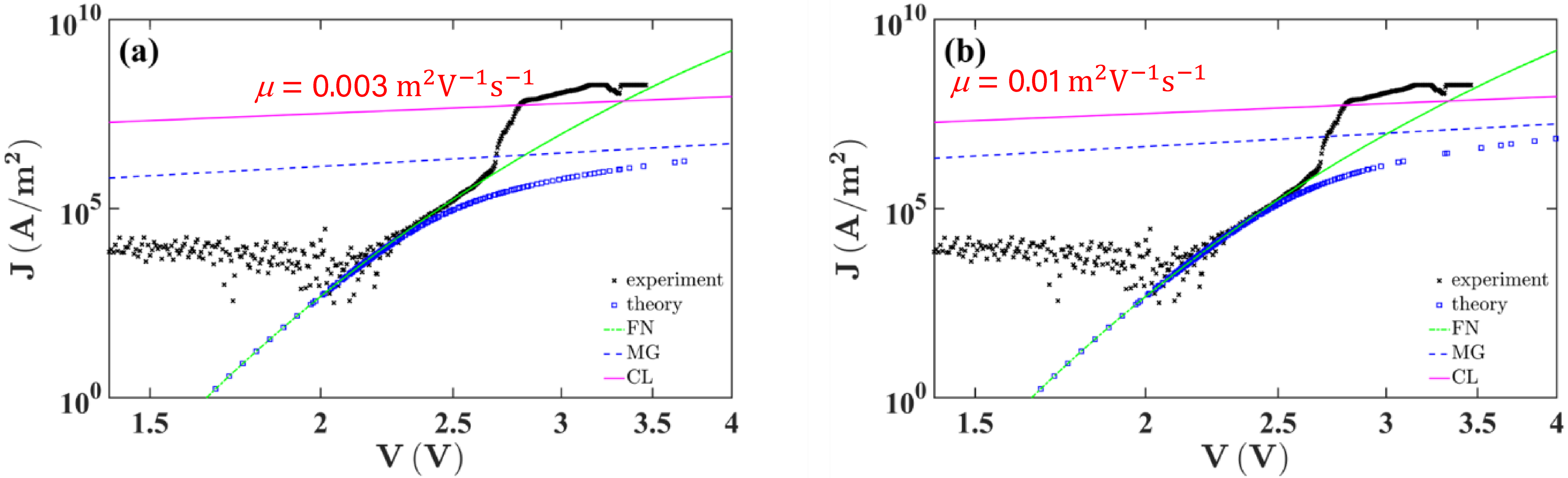

Transitions from FN to breakdown.

Conclusion

- Microscale gas breakdown theory works well with experiments.
  - Derive pin-to-plate geometry
  - Account for non-uniform space charge across the gap
- Continue nanoscale experiments
  - Account for field emission orthodoxy in FN curves
  - Characterize when space charge dominates
- Expand to include thermo-field emission in microscale gas breakdown theory and experiments
  - Leverage nexus theory
- Expand to AC fields
  - Can theory provide insight into the transitions between emission/breakdown mechanisms and frequency effects?

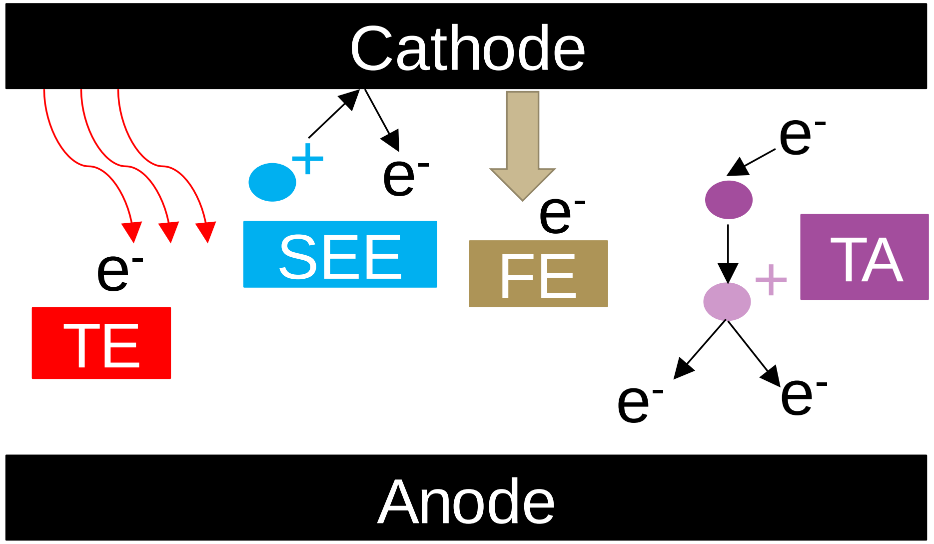

A. L. Garner, G. Meng, Y. Fu, A. M. Loveless, R. S. Brayfield, and A. M. Darr, J. Appl. Phys., Submitted.

THANK YOU

Amanda Loveless (Post-doc, NE): Theoretical Development
Russell Brayfield (PhD, AFRL): Experimental Analysis
Andrew Fairbanks (Grad Student, NE): Experimental Analysis
Adam Darr (Grad Student, NE): Quantum breakdown; Space charge theory with collisions; thermionic emission; crossed-field theory.
Harsha (Grad Student, NE): Variational calculus for space charge limited emission theory
Sarah Lang (Grad Student, NE): Liquid Emission modeling
Shengjie Gao (Grad Student, IOE): Imaging of surfaces.
Sam Dynako (Undergrad, ECE): Error Propagation of theory; Space charge theory with collisions
Caleb Darr (Undergrad, NE): Experimental Analysis; Theory of Thermionic emission.
Catherine Darr (Undergrad, AAE): Experimental Breakdown
Jacqueline Malayter (Undergrad, ECE): Work function modeling for rough surfaces.
Lorin Breen (Undergrad, NE): Modeling non-uniform microscale gas breakdown.
Weihang Li (Undergrad, AAE): Experimental Analysis